Visible spectrum quantum light sources based on $In_xGa_{1-x}N$/GaN quantum dots

Stanko Tomić,*,† Joydeep Pal,‡ Max A. Migliorato,‡ Robert J. Young,¶ and Nenad Vukmirović§

Joule Physics Laboratory, School of Computing Science and Engineering, University of Salford, Manchester M5 4WT, UK, School of Electrical and Electronic Engineering, University of Manchester, Manchester M13 9PL, UK, Department of Physics, Lancaster University, Lancaster LA1 4YB, UK, and Scientific Computing Laboratory, Institute of Physics Belgrade, University of Belgrade, Pregrevica 118, 11080 Belgrade, Serbia

E-mail: s.tomic@salford.ac.uk

Abstract

We present a method for designing quantum light sources, emitting in the visible band, using wurtzite $In_xGa_{1-x}N$ quantum dots (QDs) in a GaN matrix. This system is significantly more versatile than previously proposed arsenide and phosphide based QDs, having a tuning range exceeding 1 eV. The quantum mechanical configuration interaction method, capturing the fermionic nature of electrons and associated quantum effects explicitly, is used to find shapes and compositions of dots to maximize the excitonic dipole matrix element, and optimise the biexciton binding energy. These

*To whom correspondence should be addressed

†Joule Physics Laboratory, School of Computing Science and Engineering, University of Salford, Manchester M5 4WT, UK

‡School of Electrical and Electronic Engineering, University of Manchester, Manchester M13 9PL, UK

¶Department of Physics, Lancaster University, Lancaster LA1 4YB, UK

§Scientific Computing Laboratory, Institute of Physics Belgrade, University of Belgrade, Pregrevica 118, 11080 Belgrade, Serbia

results provide QD morphologies tailored for either bright single photon emission or entangled photon pair emission, at any given wavelength in the visible spectrum.

keywords: single photon sources, entanglement, quantum dots, correlations, III-nitrides, inverse problems.

The breakthrough in the development of solid state lighting was recently recognised by the Nobel Prize in Physics 2014 awarded to Isamu Akasaki, Hiroshi Amano and Shuji Nakamura.[1] It is important to build upon this work, and develop practical and versatile sources of quantum light, as they are key components required for the advancement of quantum photonic devices. Proof-of-principle demonstrations with InAs/GaAs,[2,3] GaN/AlN[4] and phosphide-compatible[6,7] material systems have shown that solid-state quantum dots (QDs) can be near-ideal sources of quantum light, albeit covering narrow wavelength ranges. There are many applications of quantum light beyond quantum communications at telecoms wavelengths, such as beating the classical diffraction limit in quantum imaging[8] or reducing cell damage in the microscopy of biological systems.[9] QD light sources have already been used to exceed classical optical interferometry limits,[10] but the long wavelength of emission from the InAs QDs used in this demonstration severely limited its appeal.

Radiative recombination from excitons confined in InGaN/GaN wurtzite QDs could provide versatility not afforded by other material systems, helping to target new applications of quantum photonics. Excitons in nitride quantum dots have large emission energies, unlocking the blue and ultraviolet spectral regions for quantum lights sources (QLS), which have been inaccessible to common III-V zinc-blende compatible technologies. Stronger quantum-confinement effects, resulting from their large band-gaps, band-offsets and effective masses also makes wurtzite nitride based QLS suitable for operating at higher temperatures.[4,5] Recent experiments have reported also the bound biexcitons in small III-N based QDs.[11–13] In comparison to GaN/AlN QDs,[4,14,15] the use of $In_xGa_{1-x}N$ in GaN host lattice results

in longer emission wavelengths, with the modulation of the indium content providing an additional degree of freedom required to tune the emission wavelength of photon sources throughout the visible spectral band. Also, previous reports of InGaN single QD based spectroscopy experiments,[16–18] show improved photon-correlations and extraction efficiency.[19–22] This is particularly important in applications requiring cheap, high performance single photon detectors such as visible and free-space high bandwidth quantum communications, as InGaN/GaN QDs can offer compatibility with silicon-based avalanche photodiodes.[23]

In order to design the nano-fabrication of QDs to meet the demands of specific applications, a relationship between morphology and the confined excitonic states needs to be found. This is challenging due to the effects of strain, band mixing, quantum confinement, Coulomb interactions, and correlations among particles present in the QD system. Furthermore, particle confinement in wurtzite QDs is strongly affected by large built-in electric fields induced by both spontaneous linear and non-linear piezoelectric polarizations.[24] In this letter we establish such a relationship, using the configuration interaction (CI) method, showing that emission from InGaN/GaN QDs can be optimized for both single- and entangled-photon emission throughout the visible spectrum.

The optimal QLS parameters differ depending on the type of light source required, as illustrated in Fig. 1(a) and (b). For single photon sources it is desirable to maximize the biexciton (XX) shift, so that in the two-photon cascade through the intermediate exciton (X) state, the two photons have a large spectral separation,[4] as shown in figure 1(a). Successful spectral separation of the two photons always requires an optical component, but, in practice, its specification ease of implementation are dependent on the energetic separation of the exciton and biexciton photons. At the limit of large separation an efficient, low-cost cold-mirror can be employed, whereas differentiation below <1 meV requires expensive impractical filtering.[3] The former minimizes the resources required to select emission from a single excitonic state, as the required precision in the wavelength-dependent optics reduces with increasing energy separation between the biexciton and exciton photons. On the other

hand, entangled photons can be generated through time reordering when the biexciton shift is zero,[25] as depicted in figure 1(b). We want to point out that we are not considering here entangled-photon sources scheme based on the vanishing fine structure splitting, $FSS = 0$, already realised and elaborated in the literature.[3,26,27] We focus our analysis to the time reordering scheme to generate entangled-photon pairs that require $B_{\mathrm{XX}} = 0$.[28,29]

The biexciton shift can be expressed as, $B_{\mathrm{XX}} = (E_{\mathrm{XX}} - E_{\mathrm{X}}) - E_{\mathrm{X}}$, where E_{XX} is the energy of the biexciton in its ground state, and E_{X} is the average energy of the two intermediate bright exciton states. In this material system it has been shown that the internal electric field localizes the electrons at the top, and holes at the bottom of the dot.[30] As a consequence of this charge separation, the repulsive $e-e$ and $h-h$ Coulomb interactions rapidly dominate as the dot height increases, leading to an increase in the biexciton shift.[11,15] As the electron and hole separation increases however, the optical transition matrix element for exciton recombination, p_{X}, decreases, undesirably reducing the maximum repetition rate of the photon source.[31] Thus the two requirements for an ideal single photon source, maximum intensity and spectral purity, have competing demands on the dot's height. We express this conflict in an optimization function Ξ that can be used to find the best balance between the requirements, it is defined as follows:[15,32]

$$\Xi = (E_{\mathrm{XX}} - 2E_{\mathrm{X}}) \cdot \ln\left(\frac{p_{\mathrm{X}}^{(x)}}{p_{\mathrm{X}}^{(0)}}\right), \tag{1}$$

where $p_{\mathrm{X}}^{(x)}$ is the value of the $x-$component of the dipole matrix element of the exciton transition, $p_{\mathrm{X}}^{(0)}$ is equal to $10^{-4} p_{\mathrm{X}}^{(x),\mathrm{max}}$ and $p_{\mathrm{X}}^{(x),\mathrm{max}}$ is the maximal value of $p_{\mathrm{X}}^{(x)}$ for all quantum dots considered. While the choice of $p_{\mathrm{X}}^{(0)}$ is somewhat arbitrary, we find that the positions of maxima of the optimization function are weakly dependent on its value, when it is changed within reasonable limits. Within the range of energies in which the optimization function, Eq. 1, is studied the maximum biexciton shift remains within the small limit, i.e. within an order of magnitude of the typical linewidth of emission.[3] In this limit the assumption

discussed earlier, that larger shifts are advantageous for efficient cheap filtering, holds true.

In our theoretical model the single particle electron and hole states of wurtzite $In_xGa_{1-x}N/GaN$ QDs were modelled using the 8-band $\mathbf{k}\cdot\mathbf{p}$ Hamiltonian,[15,33,34] consisting of the kinetic part that includes spin-orbit interaction, the crystal-field splitting, the strain part and additional terms arising from the presence of spontaneous and piezoelectric polarization. The strain, spontaneous, and piezo field were relaxed on augmented embedding box until convergency in several lowest electron (e) and highest hole (h) states were achieved.[15] After the single particle states were found, the (bi)exciton states were obtained using the CI method,[15,35] i.e. by direct diagonalization of the CI Hamiltonian. The many-body CI Hamiltonian contains only particle-conserving terms, and is given by

$$\begin{aligned} H &= \sum_{i}^{N_e} E_i \hat{e_i}^{\dagger}\hat{e_i} - \sum_{i}^{N_h} E_i \hat{h_i}^{\dagger}\hat{h_i} + \frac{1}{2}\sum_{ijkl}^{N_e} V_{iljk}\hat{e_i}^{\dagger}\hat{e_j}^{\dagger}\hat{e_k}\hat{e_l} \\ &+ \frac{1}{2}\sum_{ijkl}^{N_h} V_{iljk}\hat{h_i}^{\dagger}\hat{h_j}^{\dagger}\hat{h_k}\hat{h_l} - \sum_{ijkl}^{N_e,N_h} \left(V_{iljk} - V_{ikjl}\right)\hat{e_i}^{\dagger}\hat{h_j}^{\dagger}\hat{h_k}\hat{e_l}, \end{aligned} \tag{2}$$

To get excitonic states we write the Hamiltonian, Eq. (2), in a two particle basis (one electron and one hole) $|i,j\rangle = |e_i\rangle\,|h_j\rangle$, and for bi-excitons we use a four particle basis $|i,j,k,l\rangle = |e_i\rangle\,|h_j\rangle\,|e_k\rangle\,|h_l\rangle$.[36] Coulomb integrals, V_{ijkl}, required for the diagonalization of the CI Hamiltonian were evaluated in reciprocal space and then corrected using the Makov-Payne method[37] adapted for a hexagonal lattice,[15] by adding the first few terms (monopole, dipole, and quadrupole) in the multipole expansion to compensate for the effect of the mirror charges induced by periodic boundary conditions. In this way the model faithfully represents electronic and excitonic structure of a *single* QD.[15] All calculations presented here are performed with `kppw` parallel code.[38]

In our analysis of single InGaN/GaN QDs, we have assumed a hexagonal truncated pyramidal shape, most often used in the analysis of other wurtzite QD, e.g., GaN/AlN QD. Although InGaN QDs grown on the top of quantum wire (QWR) exhibit quite regular

form, it is worth pointing out that actual shape of InGaN QDs is still unclear and could alter from the perfectly symmetric one; the choice of shape here should be considered as an approximation to the real one. A model QD, in the shape of a hexagonal truncated pyramid is illustrated in Fig. 1(c). It is assumed that the QD is positioned on a wetting layer (WL) that is 0.5185 nm thick. The dimensions of the QD are controlled by two independent parameters: the diameter D of the circumscribed circle around the hexagon at the WL-QD interface at $z = 0$, and the angle between pyramid base and pyramid sides edges which is assumed to be $\alpha = 30^{\text{o}}$. The size of the QDs was controlled by D/h aspect ratio, where h is the QD height. The calculations are performed over a wide range of QDs with In content ranging from 10% to 80%. All the CI calculations involved single particle electron ($N_e = 12$) and hole ($N_h = 18$) states, including both spins.

As a first step in our optimization we calculate the biexciton shift of a variety of InGaN/GaN QD structures, and therefore assess its qualification as a QLS. One of the major shortcomings of the mean-field theories, like Hartree or Hartree-Fock approaches, is the lack of electron correlation effects, while the CI approach is capable of capturing such quantum effects explicitly. This is of paramount importance in small QDs, where the direct Coulomb integrals can be comparable in energy to the correlation effect. We have calculated for a series of smaller $\text{In}_x\text{Ga}_{1-x}\text{N}$/GaN QDs, the excitonic and biexcitonic states with In content varying from 10% to 80% and changing the QD heights in the range $h = 1 - 2.1$ nm with 0.1 nm steps, as shown in Fig. 2. The crossover between unbound to bound biexcitonic states is observed for all In compositions greater or equal to 20%, and for the aspect ratios $D/h = 4, 5, 6, 7$. As the In content reduces, the QD confinement potential for electrons and holes diminishes, leading in turn to a reduction in the number of confined states. This limits the effect of correlations, which eventually (In $< 20\%$) prevents the formation of bound biexciton.

By analysing the results presented in Fig. 2, several observations regarding the excitonic structure of $\text{In}_x\text{Ga}_{1-x}\text{N}$/GaN single QDs can be made:

1. While varying the aspect ratios (D/h) and height h, i.e. QD dimensions, for each In composition greater or equal to 20%, it was possible to identify the range of excitonic energies at which transition from unbound to bound biexciton occurs, i.e. $B_{\mathrm{XX}} = 0$. This is important as such morphologies are suitable to fulfil the criteria for the operation of entangled photon sources.

2. By moving from smaller (right side of the traces) to larger QDs (left side of the traces) it can be observed that smaller QDs support bound biexcitons while large do not. Small QDs produce less strain due to smaller volume and consequently the smaller piezoelectric field around them, with less ability to reduce the overlap between electron and hole wave function. Good overlap between wave functions produce strong correlation that in turn makes the biexciton bound. With increasing QD size more states can be confined, contributing more towards correlation and we observe characteristic minima in B_{XX} for certain QD sizes and for In content between 30% and 60%. For large QDs the piezoelectric field becomes so strong that the overlap of wave functions is strongly reduced and in this way the correlation effect is reduced as well. In such QDs the correlation effect is not strong enough any more to overcome the $e - e$ and $h - h$ repulsive interactions in a biexciton leading to its unbound character. In Fig. 4 the top line shows the exciton emission energy and indium contents that satisfy the $B_{\mathrm{XX}} = 0$ condition.

3. For certain aspect ratios from the $D/h = 5, 6, 7$ range and In contents of 40%-50%, we observe a sudden drop in B_{XX} and strongly bound biexcitons. This phenomenon arises from the confinement of increased number of states (particularly in VB where h states exhibit much larger density of states due to larger effective masses) with small variation in QD dimensions, that lead to increased correlations. However, for QDs with large In content (70%) the effect of internal electric field dominates and destroys the conditions for strong correlations as explained in 2. In QDs with smaller In content of 20% and

30%, such effect is not observed because of two reasons: a) such QDs exhibit shallower confinement with much less bound states capable of contributing to correlations and b) smaller amount of In in QD results in smaller effect of internal electric field on wave functions overlap within QD structures.

4. Also, we want to highlight that for the case of 50% In content and aspect ratio $D/h = 5$ we observe 5 crossings between bound and unbound states over the range of 30 meV of excitonic energies from $E_{\mathrm{X}} = 2.60$ eV to $E_{\mathrm{X}} = 2.62$ eV, see inset in Fig. 2. This is the region with most suitable morphology for entangled photon source devices.

In the supporting material all morphologies that exhibit $B_{XX} = 0$ in figure 3 are listed, together with excitonic energy deviation from the excitonic energy at which $B_{XX} = 0$.

After identifying suitable In contents, we proceed now with the optimisation of single QDs for single photon source (SPS) devices. For QDs with the In content in the range from 20% to 70%, the aspect ratio in the range $D/h = 6 - 11$, and the QD height in the range $h = 1$ nm to $h = 6$ nm, we have calculated the excitonic ground state energy, E_{X}, its dipole p_{X}, the biexcitonic energy E_{XX} and the optimisation function Ξ, Eq. 1. The results of the optimisation procedure are given in Fig. 3. We have observed that for each In concentration it is possible to identify a maximum in function Ξ. QD morphologies that support these maxima will provide the best SPS devices at particular wavelengths. Optimisation function Ξ, Eq. 1, assumes only the un-bound bi-excitons. However by replacing $E_{\mathrm{XX}} - 2E_{\mathrm{X}}$ with $|E_{\mathrm{XX}} - 2E_{\mathrm{X}}|$, the search can be extended to bound bi-excitons as well. We have found local maxima of Ξ in that region to be negligible. In Fig. 4 we plot the exciton energy (wavelength) vs. In concentration for the most optimal SPS QDs. The dimensions of those QDs, i.e., aspect ratio, height in nm, and In concentrations together with the emitting wavelengths in μm are: (6, 2.6, 20%, 0.401), (9, 2.1, 30%, 0.439), (7, 2.2, 40%, 0.466), (7, 2.4, 50%, 0.539), (7, 2.2, 60%, 0.603), and (7, 2.2, 70%, 0.743). On the other hand for very small QDs with $D/h = 4$ and 5, B_{XX} is small so that local maxima for these aspect ratios are lower than the one for $D/h = 6$; in addition bi-excitons become bound before Ξ can reach local maxima for

all In concentrations considered. In the supporting material all morphologies that exhibit maxima in figure 3 are listed, together with their emission wavelengths. From Fig. 4 it is clearly seen that with suitable modulation of the In content and careful design of QD dimensions, it is possible to achieve the $In_xGa_{1-x}N/GaN$ QD based SPS emission in the range from: $\lambda_{\min} = 0.403$ μm to $\lambda_{\max} = 0.754$ μm that covers the entire visible spectrum.

Recently, Deshpande et al.[20] realize good quality electrically injected single photon sources based on InGaN quantum dots in GaN nanowires. The dots in Ref.[20] have the height of 2 nm and diameter of about 25 nm. Our results indicate that optimal dot dimensions are typically slightly larger than 2 nm and therefore agree with the fact that good quality single photon sources were realized in Ref.[20] with dots of similar dimensions.

In addition to the emission wavelength other factors, such as the repetition rate, the output coupling efficiency and coherence of the emission, need to be taken into consideration in the design of SPS sources. We have estimated, from the exitonic lifetime in InGaN QDs, that the repetition rate of our SPS sources will be in the ∼GHz range. Purcell enhancement in an optical cavity could increase this even further.[41] As-grown QD typically have poor output coupling efficiency, which however could be rectified with structural engineering.[42] The emission from QDs can be highly coherent,[43] although many applications of quantum light don't require coherency of light. Also, it is very likely that the addition of the Al in the barrier material, i.e., InGaN/AlGaN QD system could provide for better thermal characteristics due to lager confinement potentials for electrons and holes, leading further toward higher temperature operations.

In summary, we have shown that with suitable variation of the In/Ga ratio in single $In_xGa_{1-x}N/GaN$ QDs it is possible to tune both SPS and entangled photon emission covering the whole visible spectrum. Using the CI method, including the effect of electron exchange and correlations interactions, we have shown that in small QDs, the exchange-correlation effect is sufficient enough to compensate for the increase of the direct Coulomb energy of two excitons in a QD. Since InGaN material have smaller piezoelectric and spontaneous po-

larization effects than in GaN, the exchange-correlation effect is capable of simultaneously reducing the electron-hole attraction (and exchange-correlation) and increasing the pairwise Coulomb repulsion. It is currently thought that InGaN QDs are formed as local composition fluctuations in quantum wells. While it is unlikely that such structures provide the level of control over QD morphology required to optimize SPS and entangled photon devices for planar structures, InGaN QDs formed in GaN nanowires present a promising alternative system where good SPSs have already been realized.[20,22,39,40] Our designs can serve as a guidance of further development of this technology. In combination with recent work optimizing the brightness,[41] efficiency[42] and coherence of light from quantum dots,[43] the results presented here can be used to design light sources for a number of applications including quantum imaging and communications.

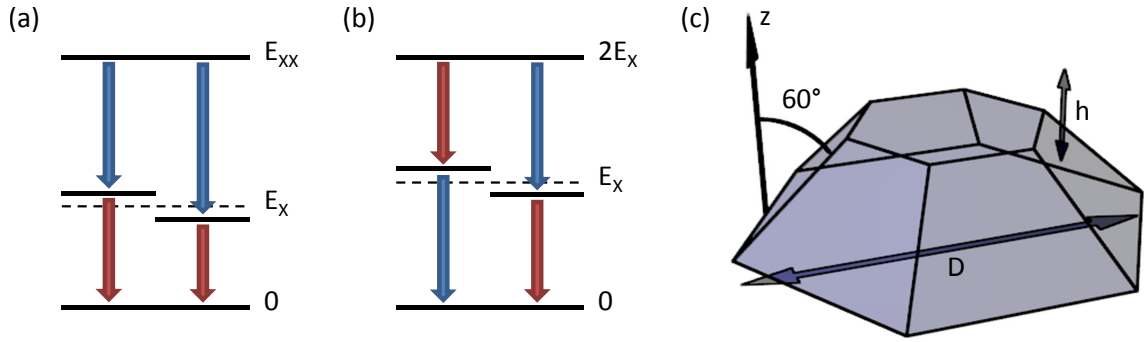

Figure 1: Simple energy level diagrams depicting the two-photon biexciton (XX) cascade through the bright intermediate exciton (X) states with; (a) a large biexciton shift, allowing photons from the biexciton and exciton states to be easily separated and, (b) zero binding energy, a condition allowing entangled photon generation through time reordering. (c) An illustration depicting the hexagonal based geometry of the quantum dot used in our calculations.

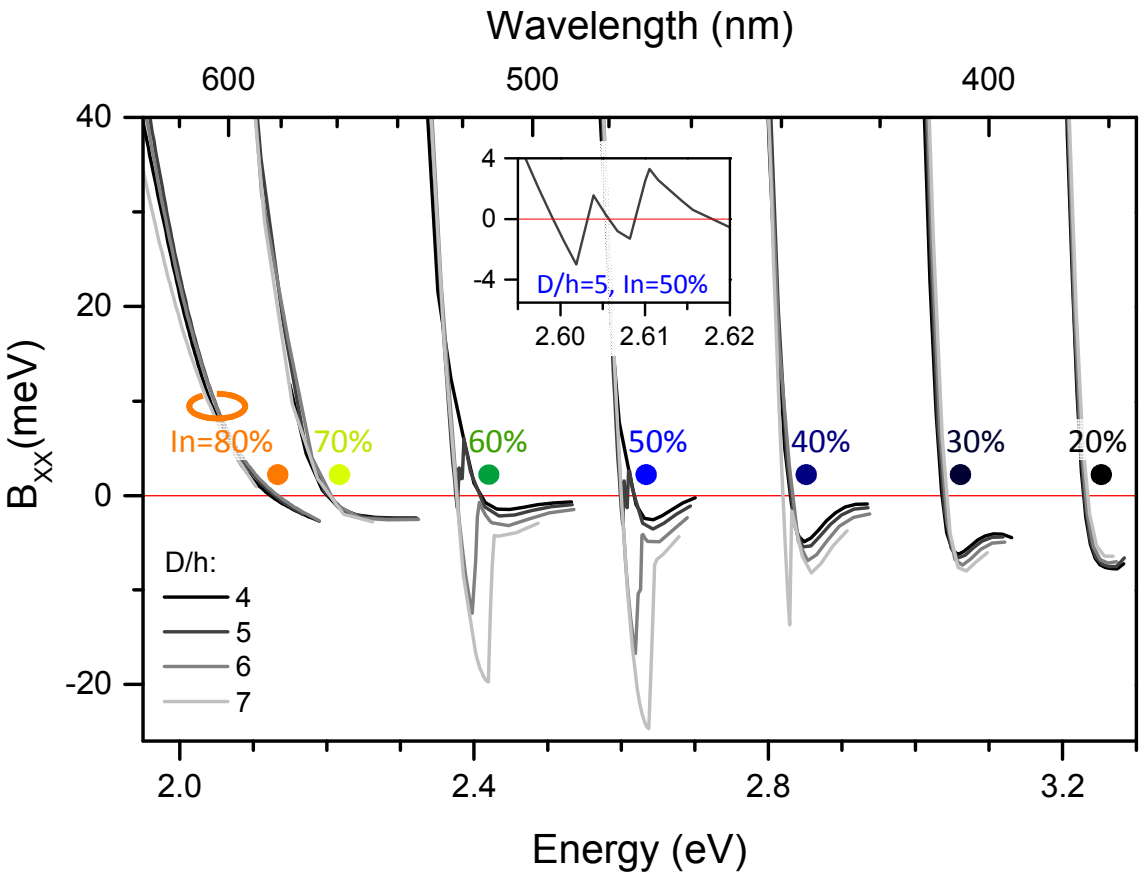

Figure 2: The biexciton binding energy as a function of the exciton's emission energy for different indium concentrations in the quantum dot and diameter/height (D/h) ratios, as labelled. The coloured circles roughly indicate the wavelength of emission at zero binding energy for each indium composition. The inset highlights the case for $D/h = 5$ and 50% indium composition, showing 5 energies at which the biexciton shift crosses zero.

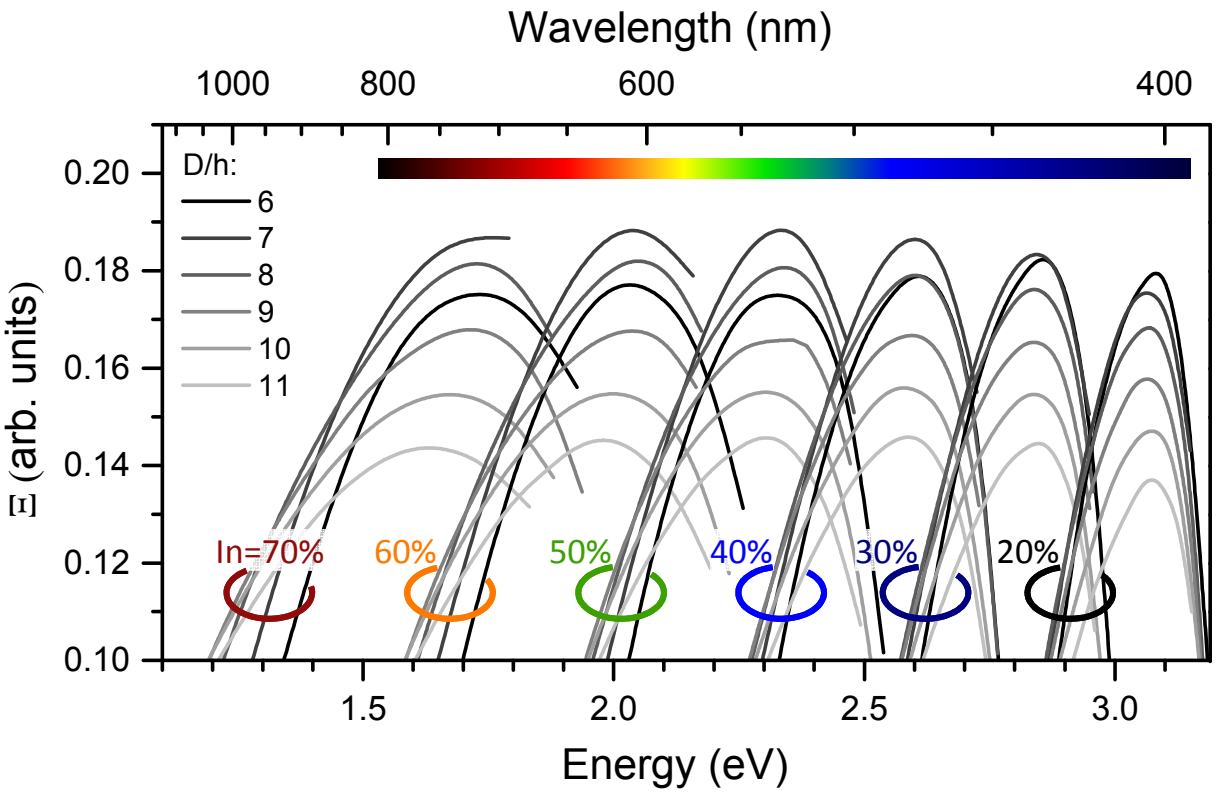

Figure 3: The dependence of the optimisation function Ξ, Eq. 1, defined in the text, on exciton emission energy for different indium concentrations in the quantum dot and diameter/height (D/h) ratios, as labelled. The coloured circles roughly indicate the wavelength of emission at which Ξ is maximised for each indium composition.

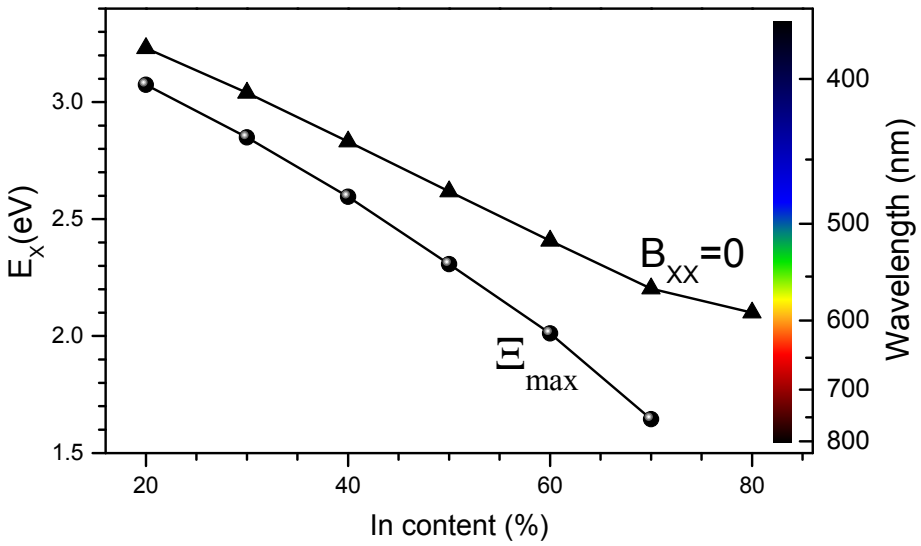

Figure 4: Exciton emission energy plotted as a function of indium composition at the point at which the optimization function (Ξ) is maximized (circles), and at the points where the biexciton shift is zero (triangles).

Acknowledgement

ST wishes to thank the Royal Society, London, grant "High Performance Computing in Modelling of Innovative Photo-Voltaic Devices," EU-COST project MP1406, and to the STFC, UK, for providing the computational resources. JP wishes to thank EPSRC for Doctoral Prize Fellowship. RJY acknowledges support by the Royal Society through a University Research Fellowship (UF110555). NV was supported by European Community FP7 Marie Curie Career Integration Grant (ELECTROMAT) and Serbian Ministry of Education, Science and Technological Development (project ON171017). The authors wish to thank Mark Holmes for valuable suggestions and discussions.

Supporting Information Available

Supporting information document listing all relevant information of QD morphologies required for the optimal SPSs and entangled-photon sources is available in separate file. This information is available free of charge via the Internet at http://pubs.acs.org/photonics. This material is available free of charge via the Internet at `http://pubs.acs.org/`.

References

(1) "The Nobel Prize in Physics 2014". Nobelprize.org. Nobel Media AB 2014. Web. 28 Jan 2015. http://www.nobelprize.org/nobel_prizes/physics/laureates/2014/

(2) Michler, P.; Kiraz, A.; Becher, C.; Schoenfeld, W. V.; Petroff, P. M.; Zhang, L. D.; Hu, E.; Imamoglu, A. A Quantum Dot Single-Photon Turnstile Device. Science **2000**, 290, 2282-2285.

(3) Stevenson, R. M.; Young, R. J.; Atkinson, P.; Cooper, K.; Ritchie, D. A.; Shields, A. J. A semiconductor source of triggered entangled photon pairs. Nature **2006**, 439, 179-182.

(4) Kako, S; Santori, C; Hoshino, K.; Gotzinger, S.; Yamamoto, Y; Arakawa, Y. A gallium nitride single-photon source operating at 200 K. Nature Materials **2006**, 5, 887-892.

(5) Holmes, M. J.; Choi, K.; Kako, S.; Arita, M.; Arakawa, Y. Room-Temperature Triggered Single Photon Emission from a III-Nitride Site-Controlled Nanowire Quantum Dot. Nano Letters **2014**, 14, 982-986.

(6) Benyoucef, M.; Yacob, M.; Reithmaier, J. P.; Kettler, J.; Michler, P. Telecom-wavelength (1.5 μm) single-photon emission from InP-based quantum dots. Appl. Phys. Lett. **2013**, 103, 162101.

(7) Miyazawa, T.; Takemoto, K.; Sakuma, Y.; Hirose, S.; Usuki, T.; Yokoyama, N.; Takatsu, M.; Arakawa, Y. Single-Photon Generation in the 1.55-μm Optical-Fiber Band from an InAs/InP Quantum Dot. J. J. Appl. Phys. Lett. **2005**, 44, L620.

(8) Boto, N.; Kok, P.; Abrams, D. S.; Braunstein, S. L.; Williams, C. P.; Dowling, J. P. Quantum Interferometric Optical Lithography: Exploiting Entanglement to Beat the Diffraction Limit. Phys. Rev. Lett. **2000**, 85, 2733-2736.

(9) Giovannetti, V.; Lloyd, S.; Maccone, L. Quantum-Enhanced Measurements: Beating the Standard Quantum Limit. Science **2004**, 306, 1330-1336.

(10) Stevenson, R. M.; Hudson, A. J.; Young, R. J.; Atkinson, P.; Cooper, K.; Ritchie, D. A; Shields, A. J. Biphoton interference with a quantum dot entangled light source. Optics Express **2007**, 15, 6507-6512.

(11) Simeonov, D.; Dussaigne, A.; Butté, R.; Grandjean, N. Complex behavior of biexcitons in GaN quantum dots due to a giant built-in polarization field. Phys. Rev. B **2008**, 77, 075306.

(12) Renard, J.; Songmuang, R.; Bougerol, C.; Daudin, B.; Gayral, B. Exciton and Biexciton Luminescence from Single GaN/AlN Quantum Dots in Nanowires. Nano Letters **2008**, 8, 2092-2096.

(13) Choi, K.; Kako, S.; Holmes, M. J.; Arita, M.; Arakawa, Y. Strong exciton confinement in site-controlled GaN quantum dots embedded in nanowires. Appl. Phys. Lett. **2013**, 103, 171907.

(14) Callsen, G.; Carmele, A.; Hönig, G.; Kindel, C.; Brunnmeier, J.; Wagner, M. R.; Stock, E.; Reparaz, J. S.; Schliwa, A.; Reitzenstein, S.; Knorr, A.; Hoffmann, A.; Kako, S.; Arakawa, Y. Steering photon statistics in single quantum dots: From one- to two-photon emission. Phys. Rev. B **2013**, 87, 245314.

(15) Tomić, S.; Vukmirović, N. Excitonic and biexcitonic properties of single GaN quantum dots modeled by 8-band $\mathbf{k} \cdot \mathbf{p}$ theory and configuration-interaction method. Phys. Rev. B **2009**, 79, 245330.

(16) Moriwaki, O.; Someya, T; Tachibana, K.; Ishida, S.; Arakawa, Y. Narrow photoluminescence peaks from localized states in InGaN quantum dot structures. Appl. Phys. Lett. **2000**, 76, 2361.

(17) Schömig, H.; Halm, S.; Forchel, A.; Bacher, G.; Off, J.; Scholz, F. Probing Individual Localization Centers in an InGaN/GaN Quantum Well. Phys. Rev. Lett. **2004**, 92, 106802.

(18) Collins, D.P.; Jarjour, A. F.; Taylor, R.A.; Hadjipanayi, M.; Oliver, R.A.; Kappers, M.J.; Humphrey, C..J.; Tahraoui, A. Two-photon autocorrelation measurements on a single InGaN/GaN quantum dot. Nanotechnology **2009**, 20, 245702.

(19) Taylor, R.A.; Jarjour, A. F.; Collins, D.P.; Holmes, M.J.; Oliver, R.A.; Kappers, M.J.; Humphrey, C..J. Cavity Enhancement of Single Quantum Dot Emission in the Blue. Nanoscale Res. Lett. **2010**, 5, 608-612.

(20) Deshpande, S.; Heo, J.; Das, A.; Bhattacharya, P. Electrically driven polarized single-photon emission from an InGaN quantum dot in a GaN nanowire. Nature Comm. **2013**, 4, 1675.

(21) Kremling, K.; Christian, T.; Dartsch, H.; Figge, S.; Höfling, S.; Worschech, L.; Kruse, C.; Hommel, D.; Forchel, A. Single photon emission from InGaN/GaN quantum dots up to 50 K. Appl. Phys. Lett. **2012**, 100, 061115.

(22) Kim, J-. H.; Ko, Y-. H.; Gong, S-. H.; Ko, S-. M.; Cho, Y-. H. Ultrafast single photon emitting quantum photonic structures based on a nano-obelisk. Sci. Rep. **2013**, 3, 2150.

(23) Jarjour, A. F.; Taylor, R. A.; Oliver, R. A.; Kappers, M. J.; Humphreys, C. J.; Tahraoui, A. Cavity-enhanced blue single-photon emission from a single InGaN/GaN quantum dot. Appl. Phys. Lett. **2007**, 91, 052101.

(24) Pal, J.;Tse, G.; Haxha, V.; Migliorato, M. A.; Tomić, S. Second-order piezoelectricity in wurtzite III-N semiconductors. Phys. Rev. B **2011**, 84, 085211.

(25) Avron, J. E.; Bisker, G.; Gershoni, D.; Lindner, N. H.; Meirom, E. A.; Warburton, R. J. Entanglement on Demand through Time Reordering. Phys. Rev. Lett. **2008**, 100, 120501.

(26) Akopian N.; Lindner, N. H.; Poem, E.; Berlatzky, Y.; Avron, J.; Gershoni, D.; Gerardot, B. D.; Petroff, P. M. Entangled photon pairs from semiconductor quantum dots. Phys. Rev. Lett. **2006**, 96, 130501.

(27) Juska, G.; Dimastrodonato, V.; Mereni, L. O.; Gocalinska, A.; Pelucchi, E. Towards quantum-dot arrays of entangled photon emitters. Nature Photonics **2013**, 7, 527.

(28) Reimer, M. E.; Dalacu, D.; Poole, P. J.; Williams, R. L. Biexciton binding energy control in site-selected quantum dots. J. Phys. Conf. Series **2010**, 210, 012019.

(29) Reimer, M. E.; van Kouwen, M. P.; Hidma, A. W.; van Weert, M. H. M.; Bakkers, E. P. A. M.; Kouwenhoven, L. P.; Zwiller, V. Electric Field Induced Removal of the Biexciton Binding Energy in a Single Quantum Dot. Nano Lett. **2011**, 11, 645-650.

(30) Andreev, A. D.; O'Reilly, E. P. Optical transitions and radiative lifetime in GaN/AlN self-organized quantum dots. Appl. Phys. Lett. **2001**, 79, 521-523.

(31) Santori, C.; Götzinger, S.; Yamamoto, Y.; Kako, S.; Hoshino, K.; Arakawa, Y. Photon correlation studies of single GaN quantum dots. Appl. Phys. Lett. **2005**, 87, 051916.

(32) De Rinaldis, S.; D'Amico, I.; Rossi, F. Exciton-exciton interaction engineering in coupled GaN quantum dots. Appl. Phys. Lett. **2002**, 81, 4236-4238.

(33) Winkelnkemper, M.; Schliwa, A.; Bimberg, D. Interrelation of structural and electronic properties in $In_xGa_{1-x}N$/GaN quantum dots using an eight-band $\mathbf{k}\cdot\mathbf{p}$ model. Phys. Rev. B **2006**, 74, 155322.

(34) Chuang, S. L.; Chang, C. S. $\mathbf{k} \cdot \mathbf{p}$ method for strained wurtzite semiconductors. Phys. Rev. B **1996**, 54, 2491-2504.

(35) Löwdin, P.-O. Quantum Theory of Many-Particle Systems. I. Physical Interpretations by Means of Density Matrices, Natural Spin-Orbitals, and Convergence Problems in the Method of Configurational Interaction. Phys. Rev. **1955**, 97, 1474-1489.

(36) Vukmirovć, N.; Tomić, S. Plane wave methodology for single quantum dot electronic structure calculations. J. Appl. Phys.**2008**, 103, 103718.

(37) Makov, G.; Payne, M. C. Periodic boundary conditions in ab initio calculations. Phys. Rev. B **1995**, 51, 4014-4022.

(38) Tomić, S.; Sunderland, A.G.; Bush, I. J. Parallel multi-band $\mathbf{k} \cdot \mathbf{p}$ code for electronic structure of zinc blend semiconductor quantum dots. J. Mater. Chem. **2006**, 16, 1963-1972.

(39) Ko, Y.-H.; Kim, J.-H.; Jin, L.-H.; Ko, S.-M.; Kwon, B.-J.; Kim, J.; Kim, T.; Cho, Y.-H. Electrically Driven Quantum Dot/Wire/Well Hybrid Light-Emitting Diodes. Adv. Mater. **2011**, 23, 5364?5369.

(40) Lazić, S.; Chernysheva, E.; Gačević, Ž.; Garcia-Lepetit, N.; van der Meulen, H. P.; and Muller, M.; Bertram, F.; Veit, P.; Christen, J.; Torres-Pardo, A.; Gonzalez Calbet, J. M.; Calleja, E.; Calleja, J. M. Ordered arrays of InGaN/GaN dot-in-a-wire nanostructures as single photon emitters. Proc. SPIE **2015**, 9363, 93630U.

(41) Birowosuto, M. D.; Sumikura, H.; Matsuo, S.; Taniyama, H.; van Veldhoven, P. J.; Nötzel, R.; Notomi, M. Fast Purcell-enhanced single photon source in 1,550-nm telecom band from a resonant quantum dot-cavity coupling. Sci. Rep. **2012**, 2, 321.

(42) Claudon, J.; Bleuse, J.; Malik, N. S.; Bazin, M.; Jaffrennou, P.; Gregersen, N.; Sauvan,

C.; Lalanne, P.; Gerard, J.-M. A highly efficient single-photon source based on a quantum dot in a photonic nanowire. Nature Photonics **2010**, 4, 174-177.

(43) Matthiesen, C.; Vamivakas, A. N.; Atatüre, M. Subnatural Linewidth Single Photons from a Quantum Dot. Phys. Rev. Lett. **2012**, 108, 093602.